J Mol Model (2013) 19:5245–5255
DOI 10.1007/s00894-013-1994-6

ORIGINAL PAPER

Exploration of various electronic properties along the reaction coordinate for hydration of Pt(II) and Ru(II) complexes; the CCSD, MPx, and DFT computational study

Jaroslav V. Burda · Zdeněk Futera · Zdeněk Chval

Received: 2 December 2012 / Accepted: 30 August 2013 / Published online: 15 October 2013

Abstract In the study behavior of molecular electrostatic potential, averaged local ionization energy, and reaction electronic flux along the reaction coordinate of hydration process of three representative Ru(II) and Pt(II) complexes were explored using both post-HF and DFT quantum chemical approximations. Previously determined reaction mechanisms were explored by more detailed insight into changes of electronic properties using ωB97XD functional and MP2 method with 6–311++G(2df,2pd) basis set and CCSD/6–31(+)G(d,p) approach. The dependences of all examined properties on reaction coordinate give more detailed understanding of the hydration process.

Keywords Ab initio calculations · Average local ionization energy · DFT · Reaction electronic flux · Electrostatic potential · Metallodrugs

Introduction

Organometallic complexes, which are important in anticancer treatment and contain chloro-ligand, are in cellular environment activated by hydration reaction (i.e., substitution reaction where chloro ligand is replaced by water molecule). This process is usually endothermic but its occurrence is enforced by very low concentration of chloride anions in cytoplasm of the cells [1, 2]. This process has to pass with appropriate rate constant since too slow a process is inefficient and too fast a reaction leads to activation out of cell or immediately after passing through cellular membrane. This enables the drug to bind to any 'appropriate' site of the closest biomolecule, e.g., to side-chains of amino acids, which are on the protein surface, and to form (often) irreversible coordination. Here it may not block any basic life functions and can be finally replace by expressing new unharmed biomolecule. Therefore tuning the drug activation, in the case of chloro-complexes, e.g., by the hydration reaction, is one of the key steps in successful design of new metallodrug. The activation of Pt(II) and other metallocomplexes was explored computationally by several groups recently,[3–10].

Also, the Ru(II) 'piano-stool' complexes attract a lot of attention due to their promising properties and their activation mechanism was examined in many theoretical papers, e.g., [11–19].

For the given chemical reaction a potential energy curve along the reaction coordinate (ϑ) can be determined, e.g., by the intrinsic reaction coordinate (IRC) method. Then, a reaction force F in each point of the coordinate ϑ can be defined [20] as:

$$F(\vartheta) = -\frac{\partial V(\vartheta)}{\partial \vartheta}. \quad (1)$$

Several critical points occur on the reaction force curve F(ϑ), which can divide the reaction into several areas: where a) mainly structural changes take place—from reactants to force minimum (alpha-point), b) electronic changes predominates—from force minimum to force maximum (gamma-point) and c) final structural reorganization finishes the process—from force maximum to product [21–23]. These points are shown in Fig. 1b.

J. V. Burda (✉) · Z. Futera
Department of Chemical Physics and Optics,
Faculty of Mathematics and Physics, Charles University,
Ke Karlovu 3, 121 16 Prague 2, Czech Republic
e-mail: Jaroslav.Burda@mff.cuni.cz

Z. Futera
Keio University, 3-14-1 Hiyoshi, Kohoku-Ku, Yokohama 223-8522, Japan

Z. Chval
Department of Laboratory Methods and Information Systems,
Faculty of Health and Social Studies, University of South Bohemia,
J. Boreckého 27, 370 11 České Budějovice, Czech Republic

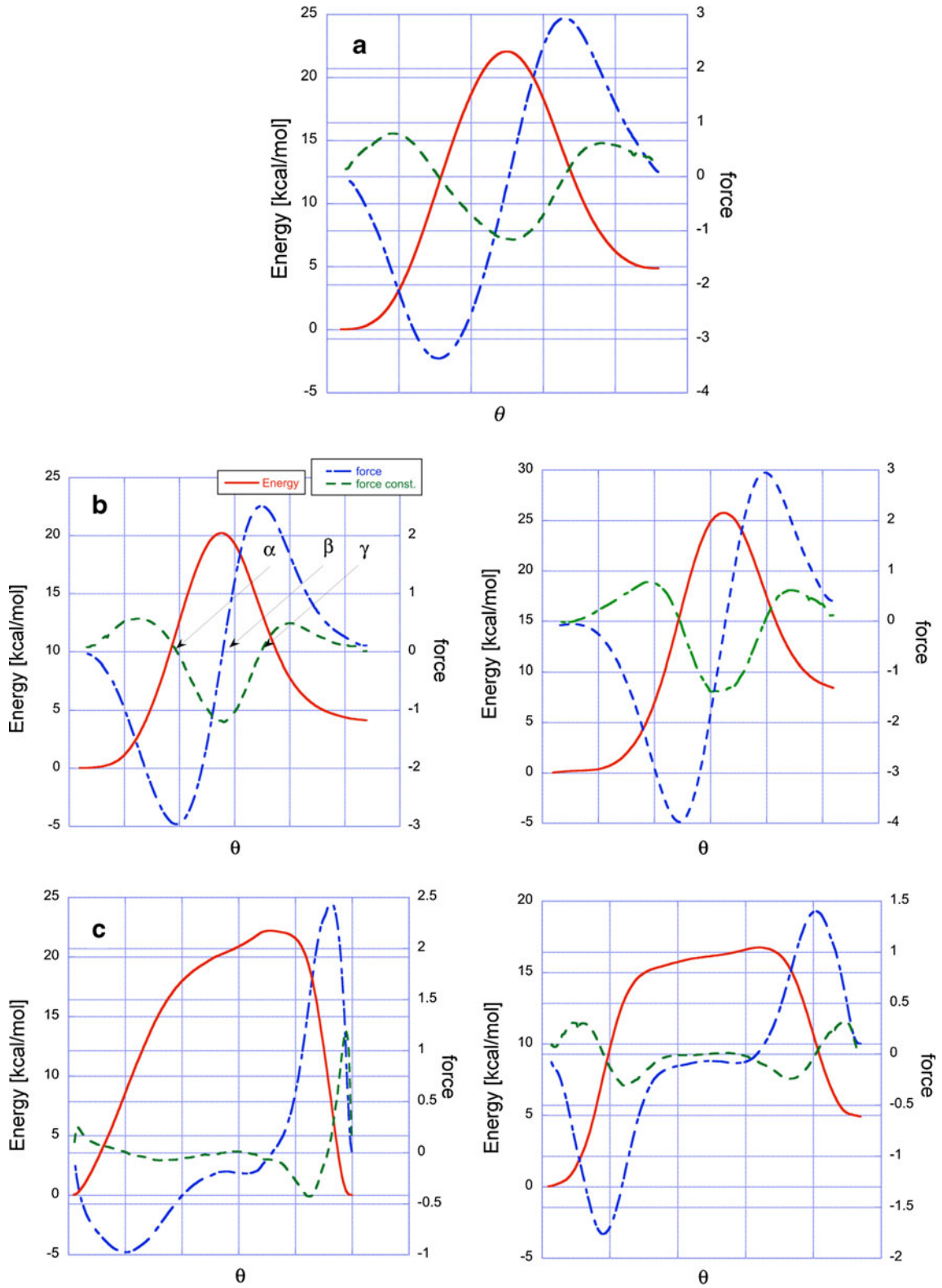

Fig. 1 PEC (red solid line), force (blue dot-dashed line) and force constant (green dashed line) for hydration process of: **a**) $[Ru(en)Cl(benzene)]^{+}$ **b**) cisplatin, and **c**) RAPTA-B complexes (by dissociative mechanism). Both dechlorination steps were considered in the cisplatin and RAPTA cases (first step left)

In a similar way to reaction force also a concept of reaction electronic flux (REF) along ϑ was introduced [24] as:

$$J(\vartheta) = -\frac{\partial \mu(\vartheta)}{\partial \vartheta}, \tag{2}$$

where $\mu(\vartheta)$ means chemical potential, which can be roughly estimated from energy of HOMO and LUMO orbitals in the individual point of IRC:

$$\mu \approx \frac{1}{2}(\varepsilon_{HOMO} + \varepsilon_{LUMO}). \tag{3}$$

It was found [25] that areas with $J(\vartheta)>0$ are connected with spontaneous electronic rearrangement indicating formation of covalent bond while $J(\vartheta)<0$ corresponds to weakening of a bond.

Important property for recognition and interaction of the given molecule in any biosystem is molecular electrostatic potential (MEP), for very instructive introduction see ref [26]. It can be defined as force acting on a positive (unit) charge located at some point in the space through the electronic charge cloud generated by the electron density and nuclei positions:

$$V(\mathrm{r}) = \sum_A \frac{z_A}{|\mathrm{R}_A - \mathrm{r}|} - \int \frac{\rho(\mathrm{r}')d\mathrm{r}'}{|\mathrm{r}' - \mathrm{r}|}. \tag{4}$$

Another tool for reactivity description of the given molecule is Average Local Ionization Energy (ALIE). It was introduced by Politzer, e.g., in refs [27, 28]

$$\bar{\mathrm{I}}(\mathrm{r}) = \sum_i \frac{\rho_i(\mathrm{r})|\varepsilon_i|}{\rho(\mathrm{r})} \tag{5}$$

in order to shed light into the location of the most reactive (easily removable) electrons. Both V(r) and $\bar{I}$ (r) are local, site-specific, properties that require the determination of electron density.

In this study we concentrate on the comparison of several different kinds of electron densities (HF, MP2, CCSD, and ωB97XD) for these descriptors evaluated along the reaction coordinate of the hydration process from the reactant system: chloro-complex + water to product state: aqua-complex + chloride. Recently we have compared the thermodynamic and kinetic parameters for hydration of $[Pt(NH_3)_2Cl_2]$ (cisplatin), $[Ru(\eta^6\text{-benzene})(en)Cl]^+$ (en = ethylenediamine, further abbreviated as Ru_en [29, 30]), and $[Ru(\eta^6\text{-benzene})(pta)Cl_2]$ complexes (labeled as RAPTA complex with pta ligand: pta=1.3.5-triaza-7-phosphatotricyclo[3.3.1.1] decane [31, 32]) [33]; their structures are drawn in Scheme 1. We reexamined the hydration process using the above-mentioned reaction descriptors for a detailed insight into the reaction mechanism.

Computational details

Since V(r) and $\bar{I}$ (r) are local properties, for which determination of an electron density is necessary, we have chosen several levels of computation for possible comparison: the MP2/6–311++G(2df,2pd), ωB97XD/6–311++G(2df,2pd) [34], and CCSD/6–31(+)G(d) methods. The (+) acronym labels a set of diffuse functions on oxygen and chlorine atoms only. The corresponding extensions for Pt and Ru pseudoorbitals by polarization and diffuse functions are taken from refs [35, 36]. For simulation of water solution the implicit solvation model (PCM) was used with cavities constructed using AU0 atomic radii. Hereafter the 6–31(+)G(d) basis set will be signed as BSOpt and the 6–311++G(2df,2pd) set as BSSP. The intrinsic reaction coordinate (IRC) calculations and optimizations were performed at B3LYP/6–31(+)G(d) level. The evaluation of MEP, ALIE, REF and some other electronic properties was done in the selected IRC points and stationary structures of the considered hydration based on the chemical reaction:

$$[Me(II)\mathrm{L_x}Cl]^{n+} + \mathrm{H_2O} -> [Me(II)\mathrm{L_x}(\mathrm{H_2O})]^{(n+1)+} + Cl^-, \tag{ch1}$$

where $n=0$ for cisplatin and RAPTA complexes and $n=1$ for Ru_en complex. For the second hydration step the first aqua ligand is replaced by $(OH)^-$ ligand in order to keep the complex during both steps electroneutral. Also, the hydroxo-aqua-cisplatin form corresponds more closely to the situation in real neutral (pH=7) solution:

$$[Me(II)\mathrm{L_x}(OH)Cl]^{n+} + \mathrm{H_2O} -> [Me(II)\mathrm{L_x}(OH)(\mathrm{H_2O})]^{(n+1)+} + Cl^-. \tag{ch2}$$

Results and discussion

Potential energy curves

For all the hydration processes the reactants and products were considered in supermolecular form. Their structures were optimized at B3LYP/BSOpt level and a correct character of minima was confirmed by diagonalization of the Hessian matrix. The same procedure was also used for determination of the TS structure and finding the appropriate vibration mode. While in the case of cisplatin and Ru_en complexes the associative interchange mechanism was considered with

Scheme 1 Structural formulas of **a**) cisplatin, **b**) Ru_en, and **c**) RAPTA-B complexes

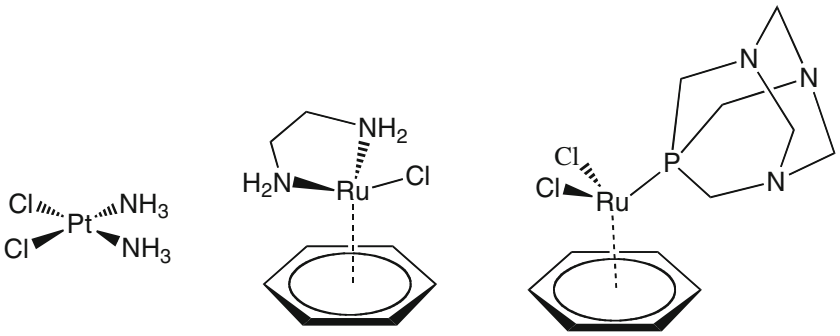

prolonged bonds to the entering and leaving ligands [37] in the case of RAPTA complex the dissociative mechanism was considered as kinetically preferable over associative one [33].

From optimized TS structures, the IRC points were obtained and potential energy curves (PEC) were constructed using the chosen computational levels. These potential curves are plotted in Figs. 1 and 2. The thermodynamic data, activation energies and rate constants were already discussed in our previous study [33]. In this contribution we will concentrate on the changes in electron densities and other above-mentioned descriptors along the reaction coordinate.

Reaction force and force constant for the CCSD/BSOpt results are plotted in Fig. 1. The alpha, beta = TS, and gamma points are marked only in Fig. 1b for clarity. It can be seen that relatively simple (textbook) behavior is displayed for the Ru_en and cisplatin complexes where activation barrier is connected with typical force shape describing single-step process and an area of negative force constant—negative eigenvalue of one vibrational mode (of antisymmetric stretching O-Me-Cl character) defines the reaction coordinate. In the case of dissociative mechanism of RAPTA, the activation exhibits a more complex course of reaction force and force constants giving the evidence of multi-step behavior. It is worth mentioning that in the RAPTA dissociative mechanism, two TS structures were localized with a stable intermediate in-between. However, none of the post-Hartree-Fock methods reproduce this picture and no stable intermediate is predicted. Instead of the first TS (TS1) maximum only a change of slope occurs leaving TS2 as a single 'true' TS structure. The existence of a stable intermediate is noticeable only at the HF and DFT levels. This can be demonstrated in Fig. 2c where PECs for the RAPTA complex are plotted. In Table 1 the activation barrier and reaction energies are collected. As compared with our previous papers [7, 33, 35] the heights of activation barriers at various computational levels can differ quite significantly. It can be noticed that HF results are quite close to CCSD values in the case of cisplatin while for Ru(II)-complexes it fails completely especially in the case of RAPTA activation energies. This is mainly due to missing description of the interaction between metal and arene [35]. The MP2/BSSP results overestimate both activation and reaction energies quite substantially in comparison with CCSD results up to 5 kcal mol^{-1}. Using smaller basis set gives much closer agreement (as is known from literature, too). As can be expected from the perturbation theory, MP3 values always improve the MP2 profile leading to usually better accord with CC method. The DFT levels (as already mentioned previously) match relatively very well the CCSD calculations with exception of the RAPTA case.

The complexity of dechlorination processes in the RAPTA complex is clearly demonstrated by more complicated shapes of force and force constant. Nevertheless, the force curves resemble, at least partially, a 'standard' behavior with both accelerating and decelerating areas separated on the reaction coordinate. From the REF values it follows that from the very beginning large decrease of bonding occurs connected with Ru-Cl bond breaking practically without any preparation phase where structural reorientation is necessary (cf. below). This is actually easy to understand since the dechlorination does not require any basic geometry changes or relaxations. The only (marginal) structural change is connected with stabilization of intermediate structure, which is represented by placing the pta and remaining chloro ligand (in first hydration step) so that the Cl-Ru-P atoms form plane perpendicular to benzene plane minimizing the steric repulsion (as already described as a necessary condition for dissociative mechanism of these complexes [33]). The RAPTA energy profiles display the highest variation of energies. While in the case of Ru_en and cisplatin all the TS energies vary within ca 6–8 kcal mol^{-1} (even including HF energies in Ru_en complex) in the RAPTA case they vary in the range of 14 kcal mol^{-1} in second dechlorination and even 17 kcal mol^{-1} in the first hydration step. Omitting HF level, the variation is still in range of 10 kcal mol^{-1} clearly pointing to high accuracy required for the proper description of these reactions.

Chemical potential and reaction electronic flux curves

For the reaction pathways the changes of chemical potential and REF are summarized in plots in Fig. 3. From the course of REF in Fig. 3 it follows that all the explored reactions start by weakening M-Cl bond. Just after the TS point, the REF curve

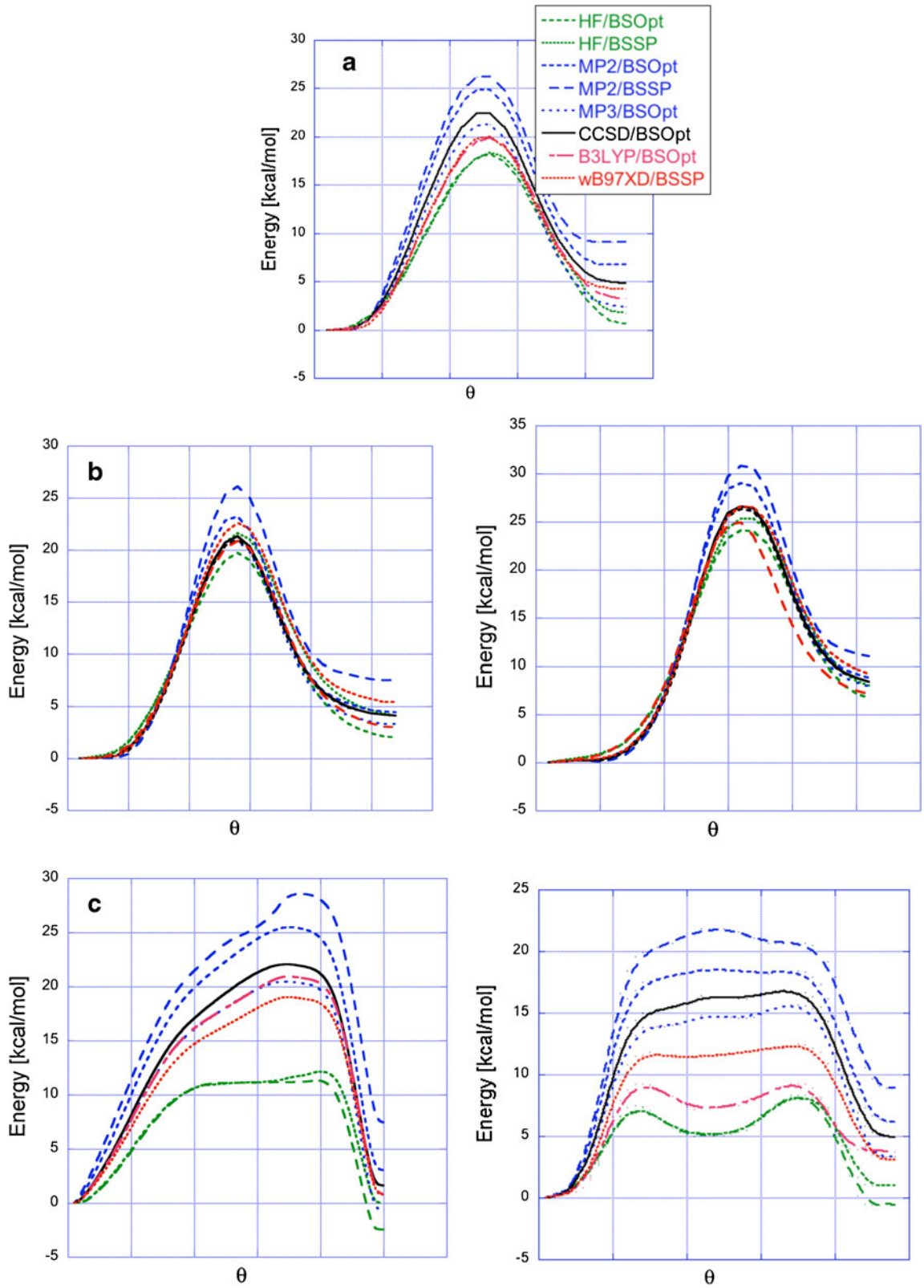

Fig. 2 Hydration energy profiles along the reaction coordinate for all the chosen computational levels. **a**) [Ru(en)Cl(benzene)]$^{+}$. **b**) cisplatin, and **c**) RAPTA-B complexes (by dissociative mechanism)

of the Ru_en complex already achieves maximum demonstrating that a new Ru-O(aqua) bond is being formed. The partially released chlorine is H-bonded simultaneously to water and en ligand. The negative area of J(ϑ) at the end of reaction is

Table 1 The height of activation barriers and reaction energies at chosen computational levels (in kcal mol^{-1})

	Ru_en		cisPt_I		cisPt_II		RAPTA_I			RAPTA_II		
	ΔEa	ΔEr	ΔEa	ΔEr	ΔEa	ΔEr	ΔEa1	ΔEa2	ΔEr	ΔEa1	ΔEa2	ΔEr
HF/BSOpt	18.2	0.6	19.7	2.0	24.1	6.7	11.0	11.6	−2.5	7.5	8.3	−0.6
HF/BSSP	18.4	1.7	21.6	4.1	25.3	8.0	11.1	12.6	0.0	7.5	8.3	1.0
MP2/BSOpt	24.8	4.8	23.2	4.4	29.0	8.8	20.5	24.1	3.0	16.8	18.4	6.2
MP2/BSSP	26.3	6.8	26.1	7.5	30.8	11.0	21.9	28.0	7.4	19.9	20.7	8.9
MP3/BSOpt	21.2	9.7	20.9	3.3	26.4	7.9	16.5	19.5	−0.7	13.8	15.7	3.3
B3LYP/BSOpt	20.0	2.8	20.9	5.2	25.9	10.5	18.7	20.6	4.1	11.9	12.6	4.6
ωB97XD/BSSP	20.1	4.3	22.6	5.4	26.6	9.2	15.1	18.4	0.8	13.4	13.6	3.1
CCSD/BSOpt	**22.4**	**2.4**	**21.3**	**4.1**	**26.6**	**8.4**	**17.6**	**20.9**	**1.6**	**15.0**	**16.7**	**4.9**
CCSD(T)/BSOpt			21.0	4.1	26.3	8.4						

connected with breaking of Cl…H(en) H-bond since the optimally coordinated aqua ligand is positioned so that it is not possible for chlorine to keep both H-bond. This relatively marginal process is clearly visible thanks to the REF behavior.

In the hydration of cisplatin the shape of chemical potential in the TS area resemble behavior of energy profile being shifted slightly toward product region clearly pointing where the largest changes of chemical potential occur. The electronic flux curves in the range of TS exhibit still weakening of bonding. This is in accord with the previously described fact that despite an associative mechanism, in the TS structures (for both first and second dechlorination) Cl and water are only very weakly bonded to central Pt atom [8] and only after TS positive area of J(ϑ) can be seen where Pt-O bond is formed.

In the RAPTA hydrations the shape of chemical potential (in accord with course of reaction force) speaks about complex course. Similarly like the energy profiles they do not reflect existence of stable intermediate that should separate two TS points. The μ(ϑ) curves exhibit one minimum. In the first dechlorination step, it is localized in the area of the TS2 structure, after which a positive area of J(ϑ) starts. It is connected with formation of Ru-O(aqua) bond. Similar conclusions hold also for the second hydration step. The most striking difference is in much narrower but substantially deeper negative course of J(ϑ) curve and much broader and lower area of positive values. Also the minimum of chemical potentials changes is 'more central' and can correspond to flatter area between both TS structures in the case of second dechlorination.

MEP and ALIE

Molecular electrostatic potential and average local ionization energy were examined on the 0.001e/Å^3 isodensity surface [38] of the individual structures. Several maxima and minima were localized on the isodensity surface of each structure. The CCSD/BSOpt level was used for further discussion. The differences of global maxima and minima (relative to corresponding absolute minimal value from the whole reaction coordinate) are plotted in Fig. 4. The absolute minima and maxima together with their relative positions on ϑ (between 0 and 1) are collected in Table 2 for the CCSD electron density. These absolute minima are localized on the released chloride anion (for MEP and ALIE of Ru_en, MEP of cisplatin, MEP and ALIE of RAPTA I and II). The only exception is the ALIE minimum in the case of cisplatin, which is located on Pt atom (cf. discussion below). Absolute maxima are located on amino groups—either of en (in Ru_en) or ammine (of cisplatin). In the RAPTA case, the MEP and ALIE maxima are localized on hydrogens of benzene ring.

Despite a 'smooth' behavior of MEP minima (MEP_min hereafter) along ϑ, the position of global minimum is relocated from water oxygen to chloro-ligand (as follows from Fig. 5a and b) in the area where ALIE_min exhibit maximal value ($\vartheta \approx 0.22$ – in relative values). For the same ϑ, also the first minimum occurs on REF curve demonstrating the decrease of Ru-Cl bonding is connected with switching the MEP_min from oxygen to chlorine region. The MEP_min becomes mildly negative before the TS is achieved clearly showing the reduction of the Cl lone-pair donation to Ru (also visible in maximal NPA partial charge δ(Ru)=0.26 e, which occurs in TS). With the consequent releasing of Cl^- from Ru(II) complex, the MEP_min value further decreases till the final value −24 kcal mol^{-1} (−1.05 eV), which is taken as relative zero. The MEP maximum (MEP_max) curve shows how the Ru(II) complex becomes 'more attractive' for nucleofiles—increasing MEP_max values in amino hydrogen area (up to 155 kcal mol^{-1}). This is a very important feature for further reactivity of these hydrated complexes. Also, the acidity of aqua proton is quite high—exhibiting the second (local) maximum in the product area of ϑ —about 144 kcal mol^{-1}. This high acidity correlates well with partial charge δ(H-aq)=0.56 e in NBO analysis; partial charges of amino hydrogens are 0.46–0.47 e.

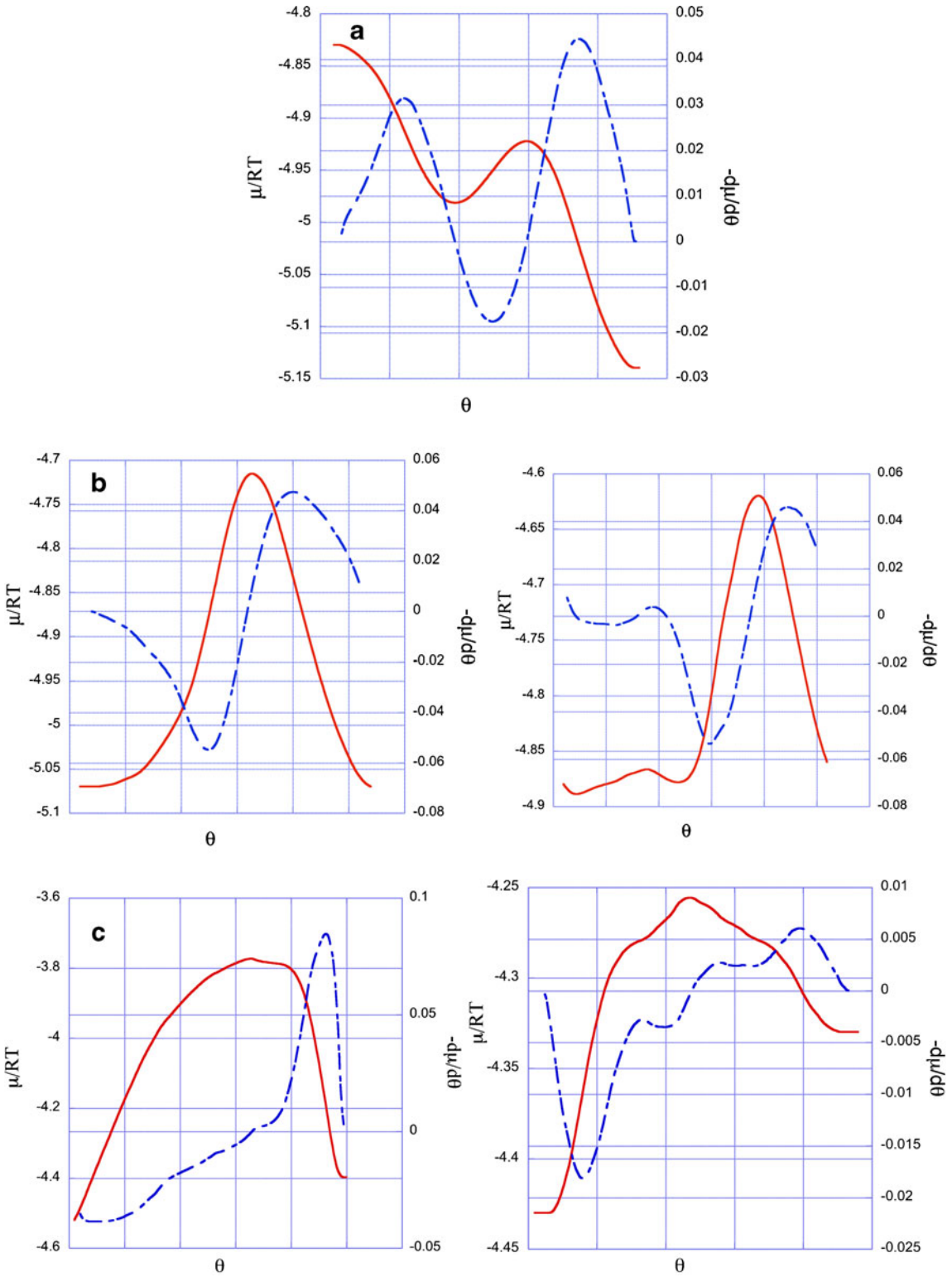

Fig. 3 Variation of chemical potential (μ/RT … red solid line) and REF ($-\frac{d\mu}{d\vartheta}$ … blue dot-dashed line) along ϑ for the complexes of: **a**) [Ru(en)Cl(benzene)]$^{+}$ **b**) cisplatin, and **c**) RAPTA-B

As mentioned above, in Fig. 4a there is a maximum of ALIE_min value of Ru_en complex at ca 1/4 of ϑ . From a closer inspection of localization of individual minima on ALIE surface along the reaction coordinate, it was found that this change is connected with relocation of maximum point localized on chlorine from the vicinity of benzene ring to the top of the complex close to approaching water molecule (cf. Fig. 6a and b). In the second part of ϑ , a minimum on the

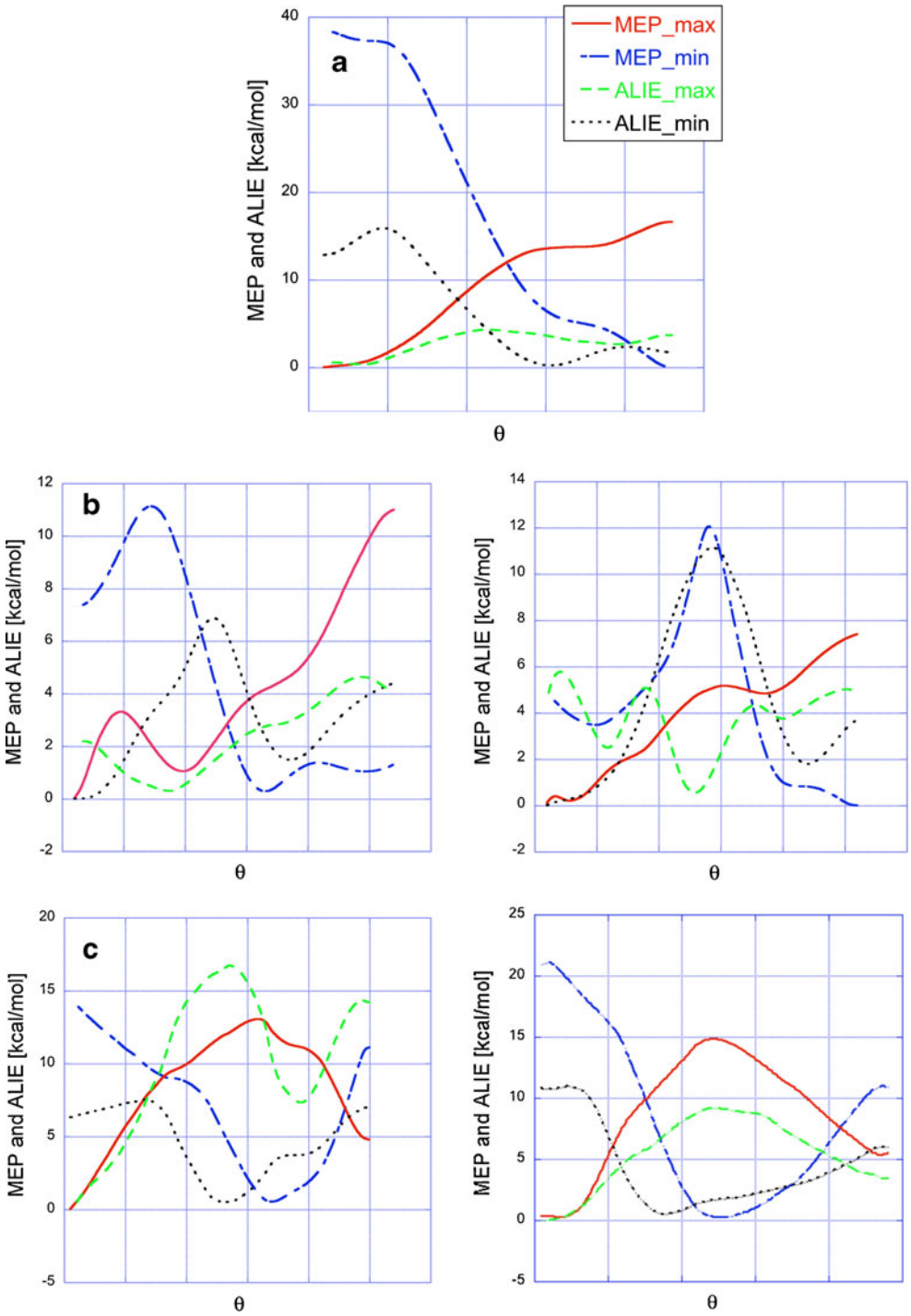

Fig. 4 Relative MEP and ALIE profiles along the reaction coordinate. MEP_max values are solid red, MEP_min blue dash-dotted, ALIE_max green dashed, and ALIE_min black dotted lines **a**) $[Ru(en)Cl(benzene)]^+$ **b**) cisplatin, and **c**) RAPTA-B complexes

ALIE curve occurs. In this case the chloride anion, where the minimum point is localized, is already relatively far from the Ru(II) complex so that minima connected with non-bonding lone pairs are practically degenerate ('averaged') without any preferred (lower) value and therefore MEP_min increases a little afterward.

In the case of cisplatin, the 1st step hydration MEP_min curve displays quite complicated character. In reactant area of ϑ the MEP_min is localized in conjunction of both chlorine atoms ca −76 kcal mol^{-1} (cf. Fig. 5c) and the second minimum on the oxygen atom is about 20 kcal mol^{-1} higher.

The ALIE_min of isolated cisplatin is connected with electron density of d_{z^2} occupied AO and it is degenerated below and above the square-planar complex as corresponds to the d_{z^2} symmetry. Due to remote water/chloride particle the symmetry of this minimum is removed and the lowest ALIE

Table 2 Absolute maxima and minima of MEP and ALIE (in eV) on the 0.001 e/Å^3 isodensity surface of the supermolecular complex and their relative position on the reaction coordinate (from 0 to 1)

		MEP		ALIE	
		min	max	min	max
Ru_en	ϑ	1.00	1.00	0.65	0.47
	energy	−1.05	6.74	11.28	20.43
cisPt_I	ϑ	0.63	0.00	0.00	0.33
	energy	−3.34	4.63	10.81	20.97
cisPt_II	ϑ	1.00	0.00	0.00	0.54
	energy	−3.18	3.93	10.36	20.70
RAPTA_I	ϑ	0.68	0.68	0.25	0.55
	energy	−3.69	3.26	9.63	18.43
RAPTA_II	ϑ	0.46	0.46	0.35	0.50
	energy	−4.06	3.24	10.82	20.38

value is 'below' square-planar complex—connected with 'bottom' d_{z^2} lobe (if water is approaching from above – cf. Fig. 6c). After TS, when the chloro-ligand is changing to chloride anion and being released under the complex plane, the global minimum is switched to 'upper' d_{z^2} lobe, cf. Fig. 6d. From this discussion follows one very remarkable fact namely that the lowest ALIE values, e.g., the place from where an electron density could be the most easily removed is not chloro-ligand but the Pt(II) orbital, which is a slightly surprising result especially because the most electronegative negative area (MEP minimum) is localized on Cl-(ligand - > anion). In the case of ALIE only the higher local minima are localized on Cl surface. This conclusion is valid for all kinds of explored electron densities - HF, MP2, DFT, and CCSD. Actually, this situation can be explained by the fact that cisplatin, and Pt(II) complexes generally, can be easily oxidized to Pt(III) and Pt(IV) more stable complexes [39]. Interestingly, MEP_min and ALIE_min maxima occur before TS, maximum of MEP_min already after α-point. From closer inspection of the electrostatic maps, it can be found that the MEP_min region starts to move from conjunction of both Cl spheres (Fig. 5c) to the top of released Cl (top in sense of continuation of Pt-Cl bond – Fig. 5d) and reaching this area after the γ -point. It should be mentioned that the MEP_min and MEP_max (in both hydration steps) remain connected with the same atom (chlorine and hydrogen of ammine group, respectively) through the whole ϑ , similarly to ALIE_min (which is localized on Pt).

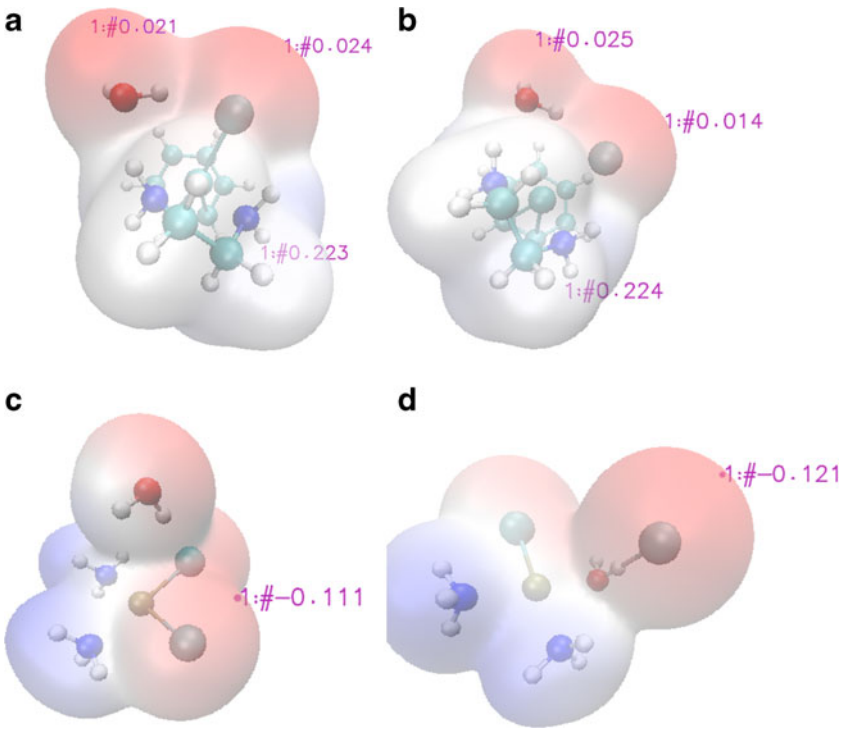

Fig. 5 MEP of **a**) Ru_en hydration process: IRC point from ϑ = 0.20 **b**) IRC point from ϑ = 0.30 **c**) cisplatin: ϑ = 0.01 **d**) ϑ = 0.97. All extremes are displayed in a.u.

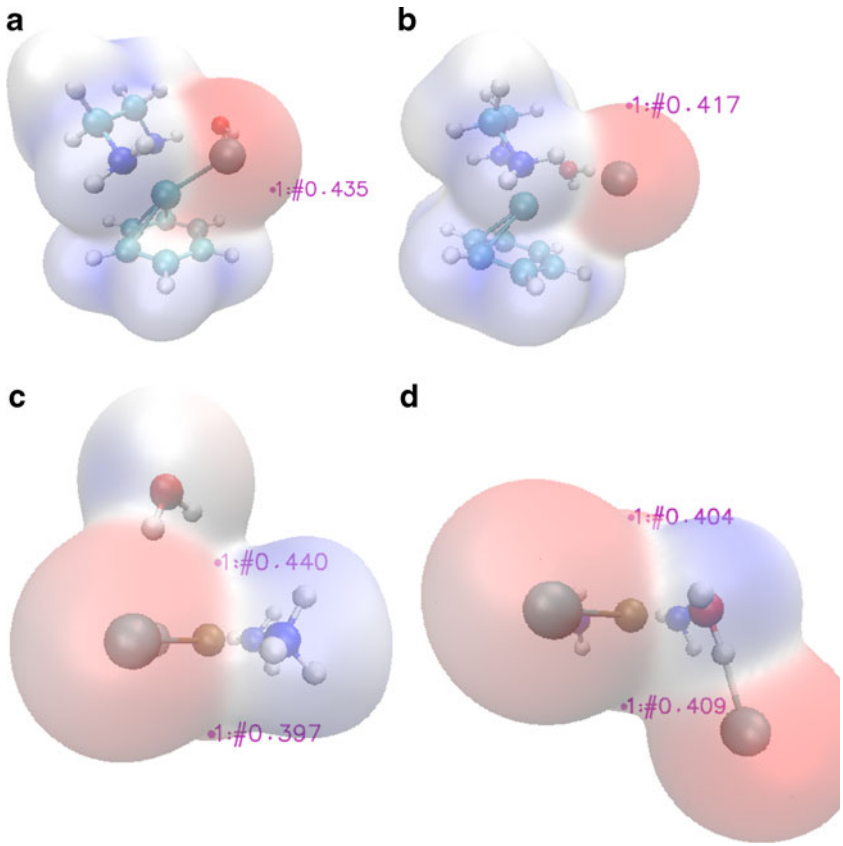

Fig. 6 ALIE surface of **a**) Ru_en hydration process: $\vartheta = 0.01$ **b**) $\vartheta = 0.55$ **c**) cisplatin hydration: $\vartheta = 0.05$ **d**) $\vartheta = 0.95$. All extremes are displayed in a.u.

The second hydration step has slightly different MEP_min preference. The global minimum is first localized on approaching water and only in the close vicinity of TS the minimum connected with chlorine starts to dominate. Similar behavior was discussed also in the Ru_en complex. As to the position on ϑ, this switching point can be roughly associated with force maximum or maximum of chemical potential. Just after TS, the (second) MEP minimum localized on water becomes finally higher than the one of hydroxyl ligand (aqua ligand from the first step). Simultaneously also the ALIE_min reaches its highest values in this region, which corresponds to the same switching of global minimum from one plane of Pt complex to the opposite one as discussed in the first hydration step. The small fluctuations of ALIE_max are basically irrelevant (this is valid for all studied reactions). They are usually caused by various polarization effects due to H-bond formation and annihilation of approaching/released water/chloride particles.

In the first hydration process of RAPTA complex, the MEP_min is, similarly to Ru_en case, localized first on oxygen of the water molecule and only after the 'TS1' structure, it is relocalized to the released chlorine. In the water coordination part of ϑ, the values of MEP_min are incresing as Ru-O bond is formed. As concerns the ALIE surfaces, one remarkable fact is that the lowest values are connected with lone pairs of one of the nitrogen atoms of PTA-ligand and only higher local minima can be associated with Cl lone pairs. This order is changed in the TS1 area and released Cl exhibits (also like in MEP) ALIE absolute minimum on the whole ϑ. The existence of both MEP_min and ALIE_min minimum inside the reaction intermediate can be explained by temporarily existence of the 'isolated' Cl…H_2O associate. When water coordinates to Ru complex it becomes much more polarized, which also increases the strength of Cl…H(aq) H-bond and in this way also the amount of Cl electron density involved in this bonding. This causes the observed increase of both MEP_min and ALIE_min values in the later parts of ϑ. However, it can be expected that this effect is model dependent and in real sample chloride will migrate to solvent, which will recover the absolute MEP_min and ALIE_min values.

Comparing both plots of Fig. 4c, it can be seen that practically the same profiles were obtained for the second hydration. In this way the discussion can be repeated also for this reaction step and it concerns not only the curve shapes but also the location of individual maxima and minima of MEP and ALIE on the isodensity surfaces.

The direct comparison of changes of chemical potential and REF along the reaction coordinate with analogous changes of MEP and ALIE is not straightforward. The main reason is that while REF and chemical potential are connected with changes of electron density during the reaction the MEP and ALIE analyses point to the places on chosen molecular surface where some 'virtual' interaction can occur—a place for possible attack by

some other species. And, of course, these places change with changing character of the complex—as a consequence of substitution reaction (hydration in these cases). In this way, the MEP and ALIE analyses of isolated reactant must be considered.

Conclusions

In this contribution we give more detailed insight into reaction mechanism of hydration/dechlorination reactions of platinum(II) and ruthenium(II) complexes studied recently. Since cisplatin and RAPTA complexes contains two chloro-ligands both dechlorination steps were considered. In RAPTA complex the dissociative mechanism is assumed as preferable where after dechlorination a stable intermediate is expected, followed by water coordination. From obtained energy profiles it is revealed that the existence of stable intermediate is not predicted at all computational levels but only at the HF (both basis sets) and B3LYP/BSOpt level used for optimization and IRC construction. From the MEP and ALIE shapes it can be found that changes occur either by switching location of global minima from one atom to another (when different 'local' minimum starts to dominate) or by shifting these locations on the surface from one part (close to some ligands) to another. All these changes occur or start and end in the region of specific key points of ϑ - α, β=TS or γ -point.

Acknowledgments Authors are grateful to Grant Agency of Czech Republic (GAČR) project No P205/10/0228 for supporting this study. Also, the access to the MetaCentrum computing and storage facilities (grant LM2010005) is highly appreciated.

References

1. Lippert B (1999) Cisplatin, Wiley-VCH, Weinheim, 1999
2. Zimmermann T, Leszczynski J, Burda JV (2011) J Mol Model 17: 2385–2393
3. Zeizinger M, Burda JV, Šponer J, Kapsa V, Leszczynski J (2001) J Phys Chem A 105:8086–8092
4. Raber J, Zhu C, Eriksson LA (2005) J Phys Chem 109:11006–11015
5. Robertazzi A, Platts JA (2004) J Comput Chem 25:1060–1067
6. Zhang Y, Guo Z, You X-Z (2001) J Am Chem Soc 123:9378–9387
7. Burda JV, Zeizinger M, Leszczynski J (2005) J Comput Chem 26: 907–914
8. Burda JV, Zeizinger M, Leszczynski J (2004) J Chem Phys 120: 1253–1262
9. Schroeder G, Kozelka J, Sabat M, Fouchet M-H, Beyerle-Pfnur R, Lippert B (1996) Inorg Chem 35:1647–1652
10. Lopes JF, Menezes VSD, Duarte HA, Rocha WR, De Almeida WB, Dos Santos HF (2006) J Phys Chem B 110:12047–12054
11. Gossens C, Tavernelli I, Rothlisberger U (2005) Chimia 59:81–84
12. Deubel DV, Lau JKC (2006) Chem Commun 2451–2453
13. Wang F, Chen HM, Parsons S, Oswald LDH, Davidson JE, Sadler PJ (2003) Chem Eur J 9:5810–5820
14. Chen JC, Chen LM, Liao SY, Zheng K, Ji LN (2007) Dalton Transact 3507–3515
15. Chen JC, Chen LM, Liao SY, Zheng KC, Ji LN (2009) J Mol Struct -Theochem 901:137–144
16. Chen JC, Chen LM, Liao SY, Zheng KC, Ji LN (2009) Phys Chem Chem Phys 11:3401–3410
17. Chen JC, Chen LM, Xu LC, Zheng KC, Ji LN (2008) J Phys Chem B 112:9966–9974
18. Gossens C, Dorcier A, Dyson PJ, Rothlisberger U (2007) Organomet 26:3969–3975
19. Gossens C, Tavernelli I, Rothlisberger U (2009) J Phys Chem A 113: 11888–11897
20. Toro-Labbe A, Gutierrez-Oliva S, Concha MC, Murray JS, Politzer P (2004) J Chem Phys 121:4570–4576
21. Burda JV, Toro-Labbe A, Gutierrez-Oliva S, Murray JS, Politzer PA (2007) J Phys Chem A 111:2455–2457
22. Jaque P, Toro-Labbe A (2000) J Phys Chem A 104:995–1002
23. Martınez J, Toro-Labbe A (2004) Chem Phys Lett 392:132–138
24. Duarte F, Toro-Labbe A (2011) J Phys Chem 115:3050–3059
25. Toro-Labbe A (1999) J Phys Chem A 103:4398–4401
26. Politzer P, Laurence PR, Jayasuriya K (1985) Environ Health Perspect 61:191–202
27. Sjoberg P, Murray JS, Brinck T, Politzer P (1990) Can J Chem 68: 1440–1446
28. Murray JS, Brinck T, Grice ME, Politzer P (1992) J Mol Struct -Theochem 256:29–45
29. Chen H, Parkinson JA, Parsons S, Coxal RA, Gould RO, Sadler P (2002) J Am Chem Soc 124:3064–3082
30. Morris RE, Aird R, Murdoch PD, Chen H, Cummings J, Hughes ND, Parson S, Parkin A, Boyd G, Sadler P, Jodrell D (2001) J Med Chem 44:3616–3621
31. Allardyce CS, Dyson PJ, Ellis DJ, Heath SL (2001) Chem Commun 1396–1402
32. Allardyce CS, Dyson PJ, Ellis DJ, Salter PA, Scopelliti R (2003) J Organomet Chem 668:35–42
33. Chval Z, Futera Z, Burda JV (2011) J Chem Phys 134:024520
34. Chai J-D, Head-Gordon M (2008) Phys Chem Chem Phys 10:6615–6620
35. Futera Z, Klenko J, Šponer JE, Šponer J, Burda JV (2009) J Comput Chem 30:1758–1770
36. Burda JV, Zeizinger M, Šponer J, Leszczynski J (2000) J Chem Phys 113:2224–2232
37. Chval Z, Sip M, Burda JV (2008) J Comput Chem 29:2370–2381
38. Bader RFW, Carroll MT, Cheeseman JR, Chang C (1987) J Am Chem Soc 109:7968
39. Bradáč O, Zimmermann T, Burda JV (2013) J Mol Model doi:10.1007/s00894-012-1442-z